AIR ENTRAINMENT BEHIND ARTIFICIALLY INFLATED CAVITIES

I. J. Campbell and D. V. Hilborne
Admiralty Research Laboratory
Teddington, Middlesex

INTRODUCTION

A fully developed cavity can be formed behind an obstacle moving through water either by boiling of the water in the low-pressure region round and behind the obstacle or by the injection of air behind the obstacle. The use of air injection can greatly extend the conditions of speed and free stream pressure under which well-developed cavities can be formed. The air is, of course, entrained at the rear of the cavity and left behind in the water and the air supply must be continually maintained.

The air entrainment behind artificially inflated cavities was first investigated experimentally in the Hydrodynamics Laboratory at the California Institute of Technology (1). In the Caltech experiments the cavities were formed behind a circular disc supported in a free surface water tunnel. Figure 1 shows diagrammatically how the entrainment rate was found to vary with the cavitation number, other parameters being held constant. The part of the curve where the entrainment is nearly constant was observed to correspond to a configuration in which a re-entrant jet or splash was formed at the rear of the cavity; in these circumstances it was supposed that the water entering the cavity collected air by turbulent entrainment and carried it downstream in falling back through the cavity wall. In the region in which Q increases rapidly with decreasing σ a pair of air-filled vortex tubes was observed trailing behind the cavity and it was supposed that the vortex cores acted as pipes along which the air was readily transported away from the cavity. From analysis of a number of such entrainment measurements it was found empirically at Caltech that the non-dimensional entrainment coefficient, C_{Qd}, correlated, although rather roughly, with the product σF of cavitation number with Froude number based on disc diameter. It was also found empirically that the "twin vortex" regime held sway when $\sigma F < 1$ and the "re-entrant jet" regime when $\sigma F < 1$.

A theory of air entrainment in the trailing vortex regime has been formulated by Cox and Clayden (2), who employed some of the concepts of aerofoil theory to calculate the size of the vortex cores. The theory of Cox and Clayden contains one parameter to be determined by fitting the theoretical predictions to experimental data.

The discovery at Caltech of the trailing vortex regime behind cavities and the application by Cox and Clayden at the Armament Research and Development Establishment of the concepts of aerofoil theory to this situation are the most interesting contributions which have been made to the subject of cavity gas entrainment.

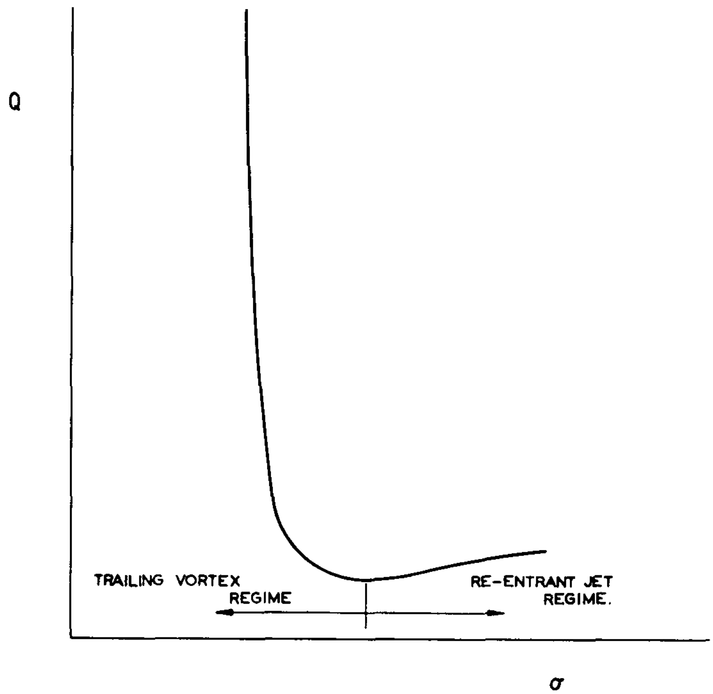

Fig. 1 - Typical entrainment curve for a cavity formed behind a given disc at a given speed

In this paper we report some air-entrainment measurements which we ourselves have made. Our experiments were very similar to those made at Caltech, but a somewhat larger range of conditions was covered. As it might be suspected that viscosity and surface tension could affect the results, the hypothesis that the entrainment depends exclusively on Froude number and cavitation number was examined in some detail. As this involved the use of models of different sizes, particular care was taken to correct for the influence of channel boundary effects.

Also we propose a modification to the theory. The theoretical model originally proposed by Cox and Clayden is not applicable to our experimental conditions. The modified theoretical model, which involves no empirical parameter,* gives predictions of gas entrainment which are in broad agreement with our experimental results.

THEORETICAL DISCUSSION

Cox and Clayden (2) point out that, since the pressure in the cavity is fairly constant, there must be a difference in the velocity on the free streamlines corresponding to the difference in hydrostatic pressure at the top and bottom of the cavity.

*We make use of some experimentally derived values of cavity dimensions but no empirical parameter which has to be evaluated from air-entrainment measurements is involved.

This gives rise to a circulation which can be evaluated. Cox and Clayden then argue that the function of the circulation is to produce a force which is equal and opposite to the buoyancy force on the bubble. This enables them to calculate the distance apart of the vortices and, thus, their inclination to the horizontal caused by the vertical velocity induced by each of them at the position of the other. They estimate the diameter of the vortex tubes from the circulation and from the condition that the pressure on their boundaries shall be cavity pressure. They then treat the vortex tubes as pipes along which the air is transported away from the cavity. In this view the air flows along each vortex tube under the action of a pressure gradient which is imposed by the hydrostatic pressure variation and so is known from the inclination of the vortices to the horizontal. The mean air velocity, v_m, in the tubes is then determined in terms of an equivalent friction coefficient, λ, for air flow in the vortex pipes. The coefficient λ is left as a parameter to be determined empirically by fitting the theoretical predictions to experimental results.

As will be seen later, application of this picture to our experimental results implies values of v_m/v_o which are in many cases less than unity. Velocity v_o is the free stream velocity, and the axial velocity of water near the vortex tubes may be supposed to be approximately v_o except in the immediate neighborhood of the bubble. When $v_m/v_o = 1$, the mean air velocity in each vortex pipe is equal to the axial velocity of the pipe walls. When $v_m/v_o < 1$, the pipe friction, far from restraining the air flow under the action of the hydrostatic pressure gradient, would actually aid it. In these circumstances the model of Cox and Clayden cannot be regarded as applicable. For this reason we propose a modification of the model. We suppose simply that when the model moves through unit distance, enough air has to be supplied to fill unit length of newly laid twin vortex trail. We now derive an expression for the entrainment on this basis.

Following Cox and Clayden and considering the vertical meridian plane through the cavity (Section AA of Fig. 2), we write

$$v_l^2 - v_u^2 = 2g(H_\ell - H_u)$$

where v_l and v_u are the velocities and H_ℓ and H_u the hydrostatic heads of water on the upper and lower surfaces of the cavity. The circulation, Γ, which is set up in this way round the cavity is given by

$$\Gamma = \int_c v \, ds$$

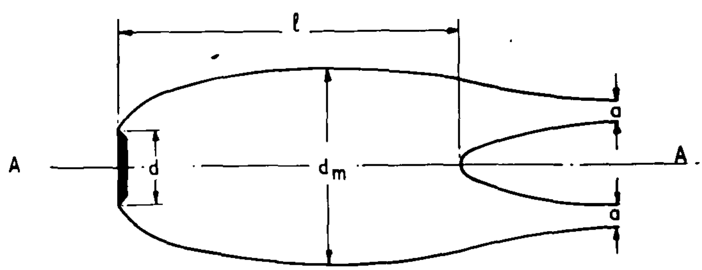

Fig. 2 - Cavity behind a disc

where C is the trace of the cavity on the vertical meridian plane. For sufficiently slender cavities this integral may be approximated as follows:

$$\Gamma = \int_C v(x)\, dx = \int_0^{\ell} (v_1 - v_u)\, dx$$

where the x axis is parallel to the direction of the main flow and ℓ (see Fig. 2) is the length of the bubble. Since

$$v_1 - v_u = (v_1^2 - v_u^2)/(v_1 + v_u) \cong (v_1^2 - v_u^2)/2v_o$$

then Γ can be further approximated:

$$\Gamma = \frac{g}{v_o} \int_0^{\ell} (H_1 - H_u)\, dx$$

$$= \frac{g}{v_o}\ \frac{\pi}{4} d_m \ell$$

where C has been approximated by an ellipse, so that the integral then becomes the area of the ellipse.

If we neglect the inclination of the trailing vortices to the horizontal and assume that the axial velocity of the water in the neighborhood of the vortices (sufficiently far downstream) is v_o, then the transverse velocity, q_C, round the periphery of the vortex tubes is given by Bernoulli's equation. Thus

$$p_C + \frac{1}{2}\rho(v_o^2 + q_C^2) = p_o + \frac{1}{2}\rho v_o^2$$

i.e.,

$$q_C^2 = v_o^2 \sigma$$

where σ is the cavitation number. In calculating q_C, Cox and Clayden allow for the inclination of the vortices and so include an additional term which has, however, only a very small influence, at least in our range of experimental conditions.

The diameter, a, of the vortex cores is then given by

$$a = \Gamma/\pi q_C$$

whence

$$a^2 = g^2 d_m^2 \ell^2/16\, v_o^4 \sigma .$$

According to our view the volume of gas entrained per unit time is given by

$$Q = 2\left(\frac{\pi}{4} a^2\right) v_o .$$

Hence the nondimensional entrainment coefficient, C_{Qd}, based on disc diameter, is given by

$$C_{Qd} \equiv \frac{Q}{v_o d^2} = \frac{\pi}{2}\left(\frac{a}{d}\right)^2 = \frac{\pi}{32}\ \frac{g^2 d^2}{v_o^4 \sigma}\left(\frac{d_m}{d}\right)^2\left(\frac{\ell}{d}\right)^2$$

or

$$C_{Qd} = \frac{\pi}{32\,F^4\sigma}\left(\frac{d_m}{d}\right)^2\left(\frac{\ell}{d}\right)^2 . \tag{1}$$

It is known from the experiments of Reichardt (3) on cavities formed behind a circular disc that

$$(d/d_m)^2 = 1.1\,\sigma$$

to a very good degree of approximation. With this approximation we can write

$$C_{Qd} = \frac{\pi}{35.2\,F^4\sigma^2}\left(\frac{\ell}{d}\right)^2 . \tag{2}$$

The ratio ℓ/d is also, of course, a function of σ for cavities behind a circular disc and so C_{Qd} is a function of F and σ. Reichardt's experiments also show that as a rough approximation we may write

$$d/\ell = 0.7\,\sigma$$

over a limited range (say $0.04 < \sigma < 0.12$). If we incorporate also this approximation we find that

$$C_{Qd} = \pi/15.8\,F^4\sigma^4 . \tag{3}$$

This makes it intelligible that it was found possible in the Caltech work to obtain a rough correlation between C_{Qd} and σF. In fact (3) is in reasonable accord with the Caltech results at the lower rates of entrainment.

EXPERIMENTAL ARRANGEMENT AND PROCEDURE

The measurements reported here were made on the small water whirling arm at the Admiralty Research Laboratory; as compared with a water tunnel of normal type this equipment offers ready dispersal of entrained air and relatively small boundary wall interference. The inner radius of the channel is 3.8 ft and the outer radius 6.8 ft; in these tests the model was positioned at the 5-ft radius. For most of the tests the model was maintained at 8-1/2 in. below the surface in water depth of 18 in. In addition some measurements were also made in different depths of water and with different vertical positions for the model.

The models consisted of a number of interchangeable discs of different diameters mounted at the front end of a sting, which was in turn carried on a supporting strut (see Fig. 3). Provision was made for air to be supplied to the back of the discs and for measurements of dynamic head and cavity pressure.

A rotating seal and conduit permitted a continuous supply of air to be brought from outside the arm to the model. A second seal was used to take a direct connection to the manometer used for measuring cavity pressure. In the case of the dynamic head, which involved measuring a wide range of pressures, a strain-gauge transducer which could be placed to take advantage of the balancing effect of radial

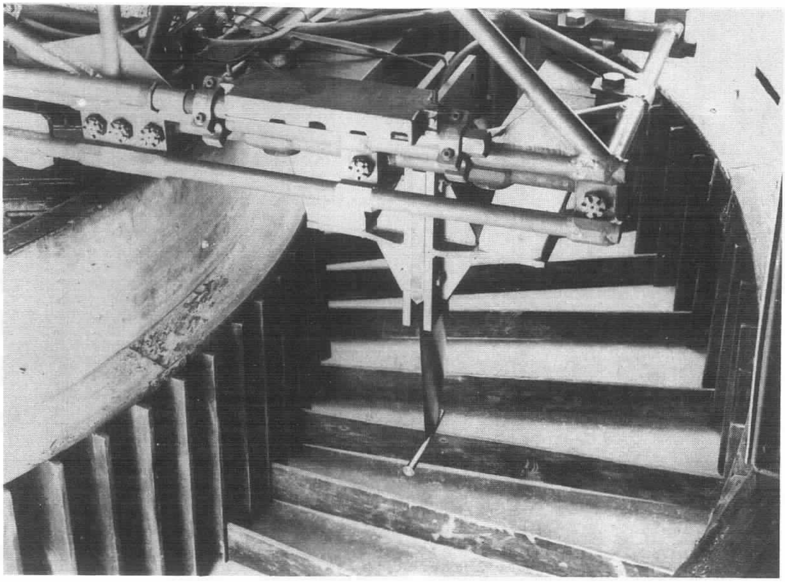

Fig. 3 - Disc (3/4 in.) mounted in position on whirling arm

acceleration was used. Pressure measurement and all filtering, metering, and control of the air supply took place off the arm.

In most cases the procedure adopted was to make a sequence of observations all at the same model speed but with differing air supply rates. Initially the air was supplied at a high rate and then the air supply valve was closed step by step, the air supply, total head, and cavity pressure being measured and the model speed checked at each stage. When eventually the cavity was on the verge of collapse, the process was reversed.

A typical example of the results obtained is given in Fig. 4. It can be seen that, as the air supply valve was closed, the cavity pressure fell steadily until a point A was reached at which a further small adjustment of the valve in the same direction caused a sharp change to conditions of lower cavity pressure as at point B. It was not found possible to hold the cavity pressure at any intermediate point by adjustment of the air supply. If the process was continued the pressure dropped until the cavity suddenly collapsed and a further large reduction in pressure occurred.

Reversing the process and re-forming a clear cavity, a similar change occurred, this time in the opposite direction and at a considerably greater rate of flow (C to D) but otherwise the results remained the same. The cavity pressure showed great sensitivity to speed fluctuation but was relatively insensitive to changes of air supply at high cavity pressures.

The right-hand section of the entrainment curve of Fig. 4 was observed to correspond to the trailing vortex regime and the left-hand section to the re-entrant jet regime. The measurements reported in this paper apply only to the trailing vortex regime. In this paper the point A has been taken as representing the transition point between the trailing vortex regime and the re-entrant jet regime.

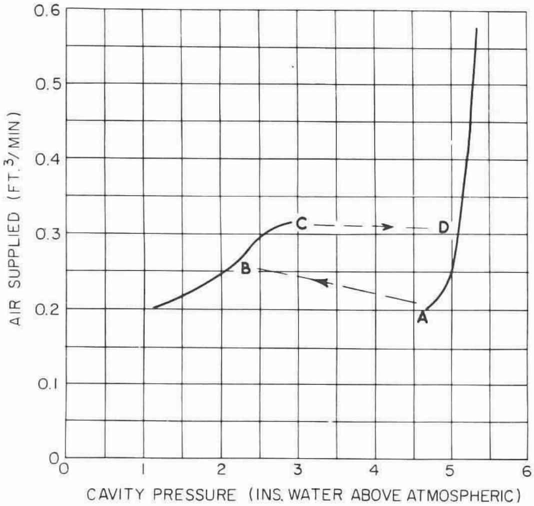

Fig. 4 - Results obtained with a 1/2-in. disc 8-1/2 in. deep with a speed of 18 fps

Figure 5 shows a photograph of a cavity with a pair of trailing vortices behind it. The appearance does not accord well with the idea of air flowing along a pipe: at least it might equally well be supposed on this evidence that the bubbles filling the tubes are simply left behind in the water.

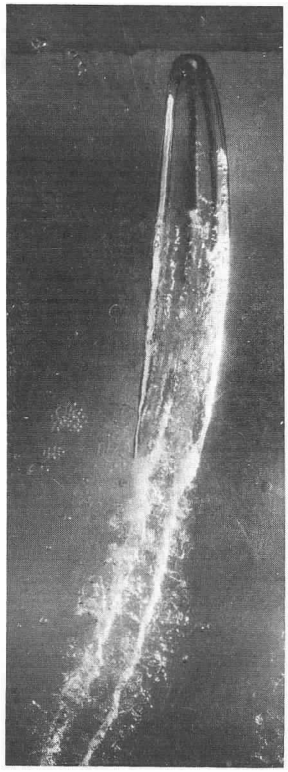

Fig. 5 - Cavity with trailing vortices

DISCUSSION OF EXPERIMENTAL RESULTS

The main results are presented in graphical form in Figs. 6 to 8, where C_{Qd} is plotted against σ for various disc sizes and for various model speeds. Individual experimental points are not plotted; in fact a great many observations were made and these define the experimental curves shown very closely. The right-hand end of each curve in Figs. 6 to 8 corresponds to the point in Fig. 4 labeled A at which transition to the re-entrant jet regime occurs.

The results presented in Figs. 6 to 8 have already been corrected for interference effects from the free surface and the channel floor. To obtain these corrections, sets of measurements were made in various depths of water, in some cases with the model held at a fixed height above the bottom and in others with the model held at a fixed depth below the free surface. It was found that for each boundary the effect of an alteration of boundary position was to move the entrainment curve bodily parallel to the axis of σ by an amount depending on the distance, expressed in model diameters, of the model from the boundary. As the effect diminishes quite rapidly with increase in distance it

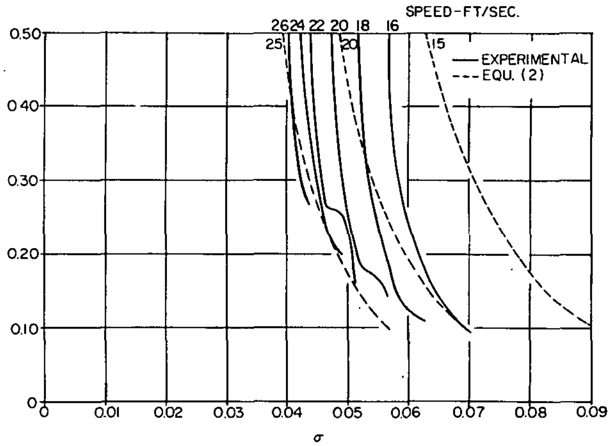

Fig. 6 - Entrainment coefficient versus cavitation number; 1/2-in. disc

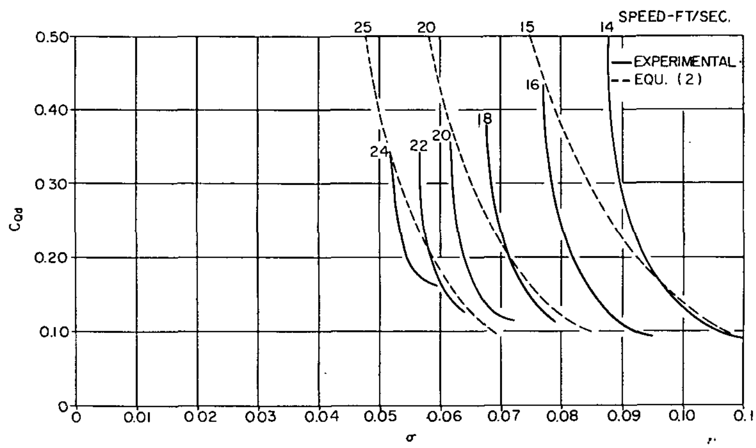

Fig. 7 - Entrainment coefficient versus cavitation number; 3/4-in. disc

was found possible to estimate the cavitation number for a given entrainment coefficient in unbounded flow, σ_0, and express the effect of boundary interference as the difference in cavitation numbers, $\sigma_0 - \sigma$. The experimental results are summarized in Fig. 9. This includes measurements made at different rates of entrainment, Froude number, and Reynolds number.

The boundary effects on entrainment are presumably associated directly with the boundary effects on the geometrical configuration of the cavity. Arguing from the theory of tunnel boundary effects on cavities and from the theory of entrainment outlined above, the proximity of a free surface might be expected at a given σ to make smaller both the cavity and the gas supply required to maintain it. In the same way

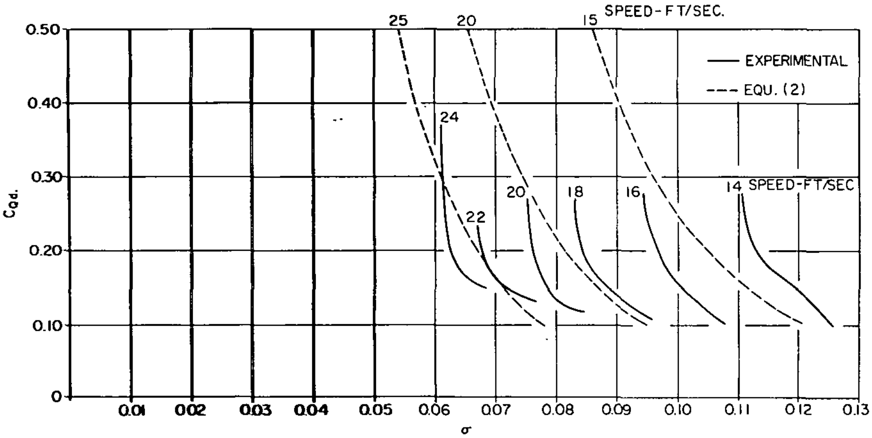

Fig. 8 - **Entrainment coefficient** versus cavitation number; 1-in. disc

the proximity of a fixed surface might be expected to have the opposite effect. This at least explains qualitatively what actually occurs. It should be noted in this connection that the bottom and sides of the channel, being covered with anti-swirl barriers, are a rather complex shape.

The distance of the nearest side wall from the model position was 14 times the diameter of the largest disc. Noting the effect of the bottom at this distance it was considered reasonable to regard boundary interference from the side walls as negligibly small.

Comparison between the entrainment curves obtained at the same Froude number but with different disc sizes shows that entrainment is not exclusively a function of F and σ. For example, the entrainment curve for the 1/2-in. disc at 18 fps is roughly parallel to the entrainment curve for the 3/4-in. disc at 22 fps but is displaced from it along the σ axis: these two cases correspond to the same Froude number. The effect is small but seems quite definite.

It appears that the entrainment curves (for the twin vortex regime) are bounded on the right by a value of σ which depends only on F. For a given value of F the entrainment curves for the larger discs lie above those for the smaller discs. Figures 10, 11, and 12 illustrate the situation.

In Fig. 10 measurements of entrainment all at the same σ are plotted against F for the different discs. The evidence is limited because it is difficult to select the data necessary for constructing such a diagram. The points clearly do not define a single curve but show a systematic trend of increasing entrainment with increasing disc size.

Again in Fig. 11, in which the minimum value of C_{Qd} capable of sustaining a cavity in the twin vortex regime is given as a function of F for the various discs, the data, although somewhat scattered, define fairly clearly, roughly parallel curves, one for each disc, and the value of minimum C_{Qd} for a given value of F increases with increasing disc size.

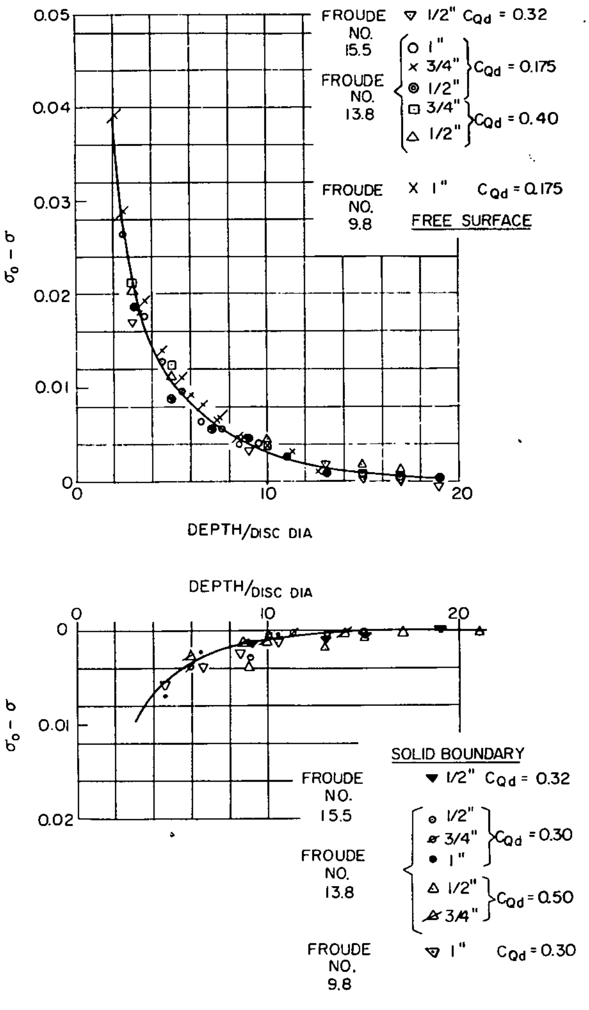

Fig. 9 - Effect of presence of channel boundaries

In Fig. 12 the highest values of σ at which a cavity with the twin vortex regime can be sustained are plotted against F for the various discs. It follows from the smallness of the scatter that σ and F are the principal factors which govern the transition condition.

A few measurements were devoted to a check on the possibility that surface tension might affect entrainment. By adding enough Teepol to the water to give an 0.043 percent solution, the surface tension was reduced from 62 dynes/cm to 43 dynes/cm, i.e., by 34 percent. When the entrainment curve for a 1/2-in. disc moving at 18 fps through this solution was compared with the corresponding curve obtained with uncontaminated water, no difference could be distinguished.

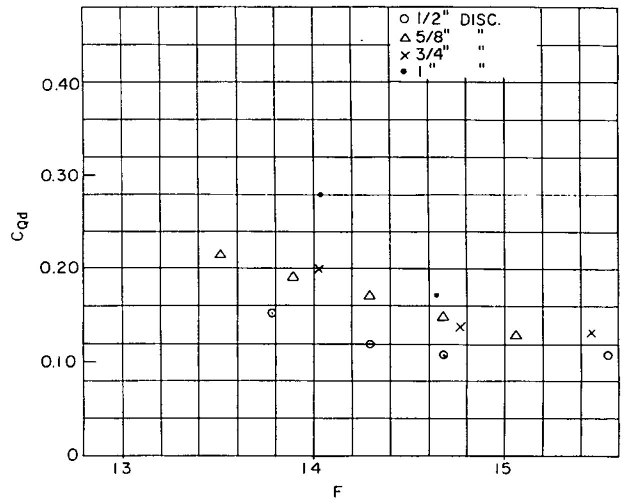

Fig. 10 - Variation of entrainment coefficient with Froude number for various disc sizes; cavitation number, 0.064

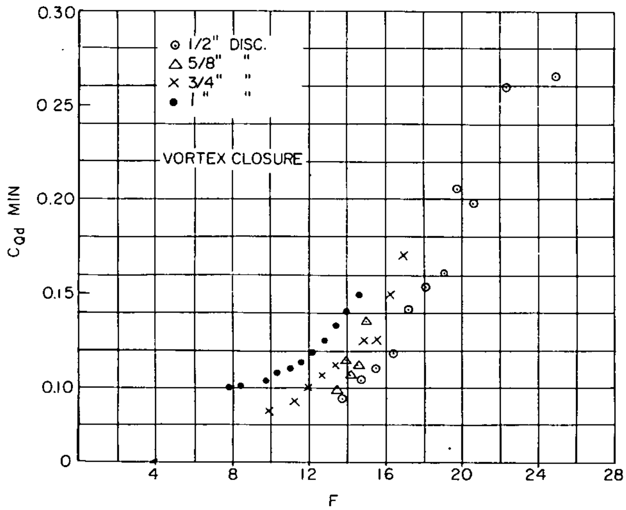

Fig. 11 - Variation of minimum obtainable entrainment coefficient with Froude number

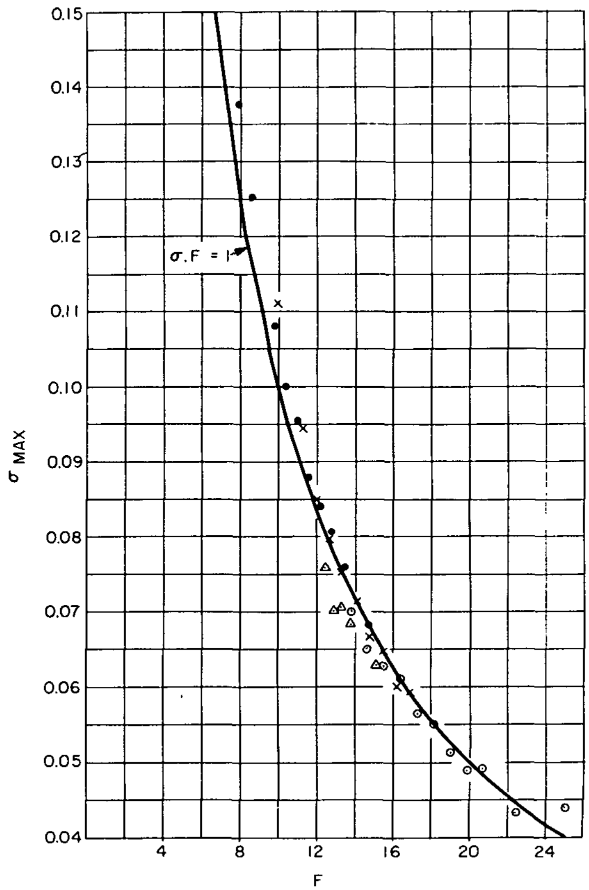

Fig. 12 - Variation of maximum obtainable cavitation number with Froude number

Accordingly it seems unlikely that the parameters, other than F and σ, on which C_{Qd} depends include the Weber number. The effects which we have described may possibly be Reynolds number effects; since the viscosity has not been varied, however, it is impossible to assert that this is the case.

The condition for transition from one flow regime to the other is extremely important. Once the trailing vortex regime takes over, the entrainment rate can rise exceedingly rapidly. It is of interest to note from Fig. 12 that the transition condition is quite well approximated by the rectangular hyperbola $\sigma F = 1$.

Finally we compare the experimental results with the theoretical predictions. In addition to the experimentally determined curves, Figs. 6 to 8 show also some corresponding theoretical curves. These have been derived from Eq. (2) using Reichardt's values of ℓ/d as a function of σ. It will be observed that the theory accounts for the measurements in broad outline.

The cases where the measured value of C_{Qd} lies below the value given by Eq. (2) are cases which would involve values of v_m/v_o less than 1 in the model of Cox and Clayden. It is for this reason that we regard the theory of Cox and Clayden as not applicable in our range of experimental conditions. The model of Cox and Clayden may, of course, be applicable and our modified version not applicable at higher entrainment rates.

The fact that the experimental results are broadly described by a theory which predicts dependence only on F and σ naturally confirms that these are indeed the main parameters on which the entrainment depends.

ACKNOWLEDGMENT

Acknowledgment is due to the Admiralty for permission to publish this paper.

NOMENCLATURE

a = diameter of vortex cores

C_{Qd} = air entrainment coefficient based on disc diameter = $Q/v_o d^2$

d = disc diameter

d_m = maximum diameter of cavity

F = Froude number based on disc diameter = $v_o/(gd)^{1/2}$

g = acceleration due to gravity

H = hydrostatic head of water

ℓ = length of cavity

p_o = free stream pressure

p_c = cavity pressure

Q = volume of air at cavity pressure entrained per second

q_C = transverse velocity at periphery of vortex core

v_o = free stream velocity

v_m = mean air velocity in vortex cores in the theoretical model of Cox and Clayden

Γ = circulation round vortex tubes

λ = equivalent friction coefficient for air flow in vortex tubes in the theoretical model of Cox and Clayden

ρ = density of water

σ = cavitation number = $(p_o - p_c)/-\frac{1}{2}\rho v_o^2$

REFERENCES

1. Swanson, W.M., and O'Neill, J.P., "The Stability of an Air-Maintained Cavity Behind a Stationary Object in Flowing Water," California Institute of Technology, Hydrodynamics Laboratory (unpublished)

2. Cox, R.N., and Clayden, W.A., "Air Entrainment at the Rear of a Steady Cavity," Proceedings of the N.P.L. Symposium on Cavitation in Hydrodynamics, London: H.M.S.O., 1956

3. Reichardt, H., "The Physical Laws Governing the Cavitation Bubbles Produced Behind Solids of Revolution in a Fluid Flow," Ministry of Supply Translation G.D.C. No. 10/5678T

* * * * *

DISCUSSION

W. A. Clayden (Armament Research and Development Establishment)

It was our experience also that for low values of C_{Qd} (say less than 0.5) the vortex tubes degenerated into trails of bubbles and it is presumably a consequence of the bubble formation that there are no effects of the hydrostatic pressure gradient along the vortex tubes. For a steady flow pattern to be maintained similar to that shown in the author's Fig. 6, the rate at which the bubbles entrain air must be equal to the rate at which the vortex tubes are laid down. For large air entrainment rates, however, fully formed tubes exist for some distance behind the cavity. In general, U_m/U_o will not be unity and in our experiments values up to 5 were measured.

It is perhaps worth pointing out that if these data are used to predict the trajectory of a missile, the air entrainment rate will be modified, since the circulation around the cavity which produces the vortices is proportional to $\cos\theta$, where θ is the angle between the longitudinal axis of the cavity and the horizontal, and also depends upon the lift force.

K. L. Wadlin (National Advisory Committee for Aeronautics)

The authors certainly have arrived at a simple relationship for the case they considered, that is, where the cavity walls are not turbulent. It would be interesting to know if the case where the cavity walls are turbulent has been considered by them. This is of interest since there is a significant difference between the character of the cavity surface shown in the photograph and that which we experience at the NACA. The photograph indicates very smooth flow along the cavity boundaries by virtue of the glassy clearness of the cavity. Our experience, at somewhat higher speeds, has been that the cavity boundary, except for an extremely small distance near its origin, is opaque, indicating turbulence. This is true with and without gas being injected into the cavity. This may mean that at low Reynolds numbers the cavity walls do not entrain the gas but only the turbulent trailing vortices, while at the higher Reynolds numbers the cavity walls would be a large factor in the entrainment process. It seems that the method of analysis used here might be extended to handle this case also.

I. J. Campbell and D. V. Hilborne

Mr. Clayden's remarks imply that, even when the trailing vortex regime holds sway, there are still two possible situations. In the one situation, at relatively low airflows, the air-filled vortex tubes break up into bubbles and this is the situation in our experiments. In the other situation, at high entrainment rates, fully formed tubes exist for some distance behind the cavity and that situation was realized in the experiments of Cox and Clayden. We agree with this suggestion.

We agree too with Mr. Clayden's remark that the air entrainment rate must be modified when the direction of motion is no longer normal to the direction of gravity and must depend also on the lift force. Appropriate experiments would be interesting.

With regard to Mr. Wadlin's comments it has been our experience that clear cavities are associated with the trailing vortex regime. The only opaque cavities which we have encountered have been associated with the re-entrant jet regime: in these circumstances the wall roughness arises from the re-entrant jet splashing onto the cavity wall. What happens in the re-entrant jet regime is outside the compass of the present paper. Light might be thrown on the point which Mr. Wadlin has raised by experiments with roughened discs behind which cavities in the trailing vortex regime are produced.

The authors wish to thank Mr. Clayden and Mr. Wadlin for their written contributions.

* * * * *